

## High- $p_T$ production of direct photons and jets in quantum chromodynamics

L. Cormell

*Physics Department, University of Pennsylvania, Philadelphia, Pennsylvania 19174*

J. F. Owens

*Physics Department, Florida State University, Tallahassee, Florida 32306*

(Received 10 March 1980)

The production of high- $p_T$  direct photons is studied using quantum chromodynamics. The theoretical predictions are shown to be compatible with the existing data over the energy interval  $20 < \sqrt{s} < 63$  GeV. In addition, the possibility of using a high- $p_T$  direct-photon trigger in hadronic-jet experiments is studied. By simultaneously triggering on a direct photon and on the away-side hadronic jet it is possible to obtain more precise information concerning the underlying dynamical subprocesses than if a two-jet trigger is used. In particular, one can, by using a combination of  $\pi^+$ ,  $p$ , and  $\bar{p}$  beams, measure both the pion quark and gluon distribution functions as well as the gluon distribution function for the proton. Furthermore, if particle identification is available for the away-side jet, one can separately measure various quark and gluon fragmentation functions. A method of measuring the  $Q^2$  dependences of these various functions is also discussed.

### I. INTRODUCTION

The pointlike nature of the photon-quark coupling makes the photon a valuable and unique probe for studying both hadronic structure as well as the interactions of hadrons. Deep-inelastic electroproduction,  $e^+e^-$  annihilation, and the hadronic production of high-mass lepton pairs have all added greatly to the present state of our knowledge of hadron dynamics.<sup>1</sup> Studies involving real photons have indicated that useful information can be gained from studying, for example, the photon structure function<sup>2</sup> and high- $p_T$  photoproduction of both particles<sup>3</sup> and jets.<sup>4</sup> Another important topic in this latter category is the hadronic production of direct (or prompt) photons at large transverse momenta.<sup>5-10</sup>

Direct photons, i. e., photons unaccompanied by additional hadrons, are interesting because they directly probe the large-momentum-transfer subprocess without the intervention of an unknown fragmentation function. In this sense they possess many of the same advantages as do jets for probing the nature of the parton-parton scattering subprocesses. Such photons have in addition the advantage that there are no questions of jet detection efficiency, quark- versus gluon-jet properties, jet-mass effects, etc., which give rise to uncertainties when interpreting conventional hadronic-jet data. Furthermore, it has long been realized that high- $p_T$  direct photons should be produced at a rate which was comparable to that of single particles, e. g.,  $\pi^0$ 's, thereby making it possible to perform high-statistics measurements with practical facilities.

In Sec. II the calculation of high- $p_T$  direct pho-

tons using quantum chromodynamics (QCD) is reviewed and compared with the existing data. Section III is devoted to a discussion of measurements involving the away-side jet in addition to the direct photon. In Sec. IV it is shown how such measurements can be used to determine various parton distribution and fragmentation functions. Our conclusions are summarized in Sec. V.

### II. DIRECT PHOTONS AND QCD

There are a variety of mechanisms for producing high- $p_T$  photons. First of all, quarks can fragment into (by bremsstrahlung) a photon and the fragmentation function can be calculated.<sup>8</sup> However, since the photon takes only a fraction of the parton's momentum this is not the most efficient way to create a high- $p_T$  photon. Furthermore, the photon will in this case be accompanied by additional hadrons from the fragmenting quark. This contribution will be suppressed by approximately a factor of  $\alpha$  with respect to the single- $\pi^0$  rate. Although this suppression will be offset somewhat by the fact that the  $q \rightarrow \gamma$  fragmentation is flatter than that for  $q \rightarrow \pi^0$ , the net contribution is still small. A second, more efficient source of photons would be any subprocess in which the photon was produced without any intermediate fragmenting quark. Such a photon would not have any accompanying hadrons and is therefore called a direct photon. To lowest order in the strong running coupling constant  $\alpha_s(Q^2)$  the two subprocesses predicted by QCD are

$$q\bar{q} \rightarrow \gamma g \quad (1a)$$

and

$$gq \rightarrow \gamma q. \quad (1b)$$

The cross-section expressions for these two subprocesses after performing color sums and spin averages are

$$\frac{d\sigma}{dt}(q\bar{q}) = \frac{\pi\alpha_s\alpha_s}{s^2} \frac{8}{9} e_i^2 \left( \frac{u}{t} + \frac{t}{u} \right) \quad (2a)$$

and

$$\frac{d\sigma}{dt}(gq) = -\frac{\pi\alpha_s\alpha_s}{3s^2} e_i^2 \left( \frac{u}{s} + \frac{s}{u} \right), \quad (2b)$$

where  $e_i$  is the fractional charge of the  $i$ th quark and  $s, t, u$  are the Mandelstam variables for the parton-parton scattering subprocess. These two subprocesses will serve as the basis for the predictions discussed in the remainder of this paper.

It is widely anticipated that at very large values of  $p_T$  the above subprocesses should dominate. However, there are several other sources of direct photons including, for example, next-to-leading-order terms. In this regard, a recent calculation<sup>11</sup> of the  $qq \rightarrow qq\gamma$  subprocess shows that it provides only a small correction to the basic 2→2 subprocesses given above. In addition, for a moderate value of  $p_T$  there can be contributions from the scattering of nonelementary fields as in the constituent-interchange model<sup>8</sup> (CIM). While these terms should be present at some level, it is difficult to properly normalize them. In particular, a recent calculation<sup>12</sup> of the  $\pi q \rightarrow \pi q$  subprocess suggests that the conventional CIM normalization may be too large by several orders of magnitude. Owing to this theoretical uncertainty in the CIM normalization, such contributions will not be included in this calculation.

In the approximation that the colliding partons are collinear in the center-of-mass frame of the colliding hadrons the direct-photon invariant cross section is given by

$$\begin{aligned} E \frac{d^3\sigma}{dp^3}(AB \rightarrow \gamma + X) \\ = \sum_{ab} \int dx_a dx_b G_{a/A}(x_a, Q^2) G_{b/B}(x_b, Q^2) \\ \times \frac{\hat{s}}{\pi} \frac{d\sigma}{d\hat{t}}(ab \rightarrow \gamma + X) \delta(\hat{s} + \hat{t} + \hat{u}), \quad (3) \end{aligned}$$

where a caret has been used to denote the Mandelstam variables for the parton-parton subprocesses. The input proton quark distributions at  $Q_0^2 = 4$  (GeV/c)<sup>2</sup> are given in Ref. 13 while the input gluon distribution is that of Ref. 14, renormalized so as to satisfy momentum conservation when used with the previously mentioned quark distributions. For  $Q^2 > Q_0^2$  the distribution functions are calculated in the usual manner in accordance with the

predictions of QCD as discussed in Ref. 13. For the pion the counting rule distributions of Ref. 15 have been used with  $Q_0^2$  changed to 4 (GeV/c)<sup>2</sup>. The value of the strong-interaction  $Q^2$  scale parameter  $\Lambda$  was chosen to be 0.4 GeV/c and the strong running coupling constant  $\alpha_s(Q^2)$  is given by  $\alpha_s(Q^2) = 12\pi/(33 - 2f) \ln(Q^2/\Lambda^2)$  with  $f=4$  being the number of quark flavors. The  $Q^2$  definition of Ref. 14,  $Q^2 = 2\hat{s}\hat{t}\hat{u}/(\hat{s}^2 + \hat{t}^2 + \hat{u}^2)$ , has been used.

For large values of  $p_T$  the above prescription is expected to yield a realistic prediction for the direct-photon yield. However, for moderate values of  $p_T$ , studies<sup>13,14,16</sup> of single-particle and jet cross sections have shown that parton transverse momenta can give rise to a smearing effect which enhances the cross section. The precise amount of this enhancement depends crucially on the detailed treatment of the parton kinematics<sup>17</sup> (on-shell or off-shell partons) and also on the manner in which the poles at  $\hat{s}, \hat{t}, \hat{u} = 0$  are avoided. Fortunately, however, the direct photon production predictions do not depend sensitively on inclusion of such smearing effects. In order to demonstrate this result the calculation has been performed both with and without the  $k_T$  smearing.

The parton  $k_T$  effects have been calculated as discussed in Ref. 18 where the average value of the parton  $k_T^2$  was approximated by a constant value,  $\langle k_T^2 \rangle = 1.0(\text{GeV}/c)^2$ . Additional details concerning the treatment of the poles in the 2→2 subprocesses may be found in Ref. 13.

Data<sup>19-22</sup> for direct  $\gamma$  production at  $\theta = 90^\circ$  are shown in Fig. 1 for several energies. We have chosen to plot the photon cross section directly rather than the  $\gamma/\pi^0$  ratio in order to avoid questions concerning the normalization of the theoretical predictions. There is a wide discrepancy among the various theoretical predictions in the literature due, in part, to different choices of the experimental  $\pi^0$  data used to normalize the theoretical  $\gamma$  predictions. In each case the data shown in Fig. 1 have been obtained by taking the experimental  $\gamma/\pi^0$  ratio and multiplying it by the  $\pi^0$  cross section obtained using the same apparatus. Thus, the relative normalization errors between the different data sets should be comparable to the relative normalization errors between the various  $\pi^0$  data sets.

The theoretical predictions obtained using Eq. (3) are shown by dashed lines in Fig. 1 while the solid lines show the result of including parton  $k_T$  smearing as discussed above. This latter effect raises the cross section only slightly in this kinematic region so that the comparison with the data does not depend strongly on the model-dependent smearing estimate. The agreement between the theoretical predictions and the data is good, con-

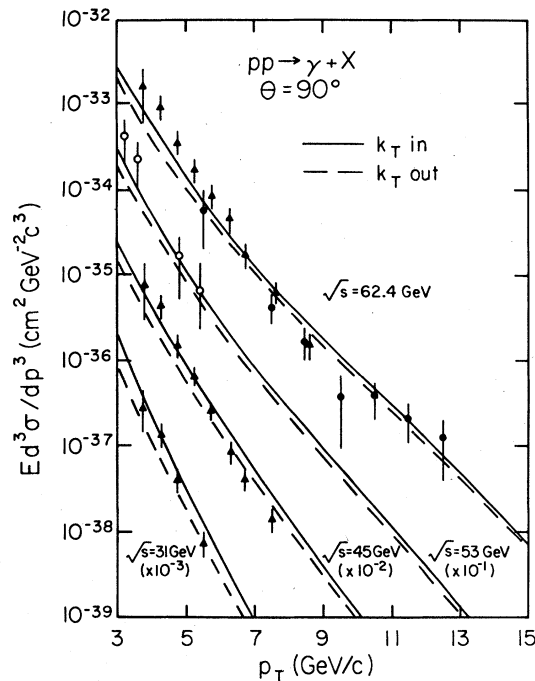


FIG. 1. A comparison between the theoretical predictions and the data for direct- $\gamma$  production at  $\theta=90^\circ$ . The data are from Ref. 19 (triangles), Ref. 20 (closed circles), and Ref. 22 (open circles). For clarity, the curves and data at  $\sqrt{s}=53$ , 45, and 31 GeV have been suppressed by factors of 10, 100, and 1000, respectively.

firming, therefore, the expectation that the lowest-order QCD subprocesses should be able to describe the large  $p_T$  production of direct photons. While this does not prove that the theory is correct, it does provide another consistency check on the theory.

Recently, additional data<sup>23</sup> on direct photon production have been obtained at lower energies,  $19.4 \leq \sqrt{s} \leq 23.7$  GeV. To increase the statistics of the data sample the  $\gamma/\pi^0$  ratio is given versus  $p_T$  subject to the constraint that the center-of-mass production angle  $\theta$  lie in the range  $90^\circ \leq \theta \leq 160^\circ$ . Also,  $\pi^0$  data in the same kinematic range have been obtained using the same apparatus.<sup>24</sup> The unfolded photon cross section, integrated over the angular range given above, is shown in Fig. 2. The dashed lines show the predictions of Eq. (3) while the solid lines have the parton  $k_T$  smearing included. In both cases the theoretical predictions have been integrated over the same angular region covered by the data. At these lower values of  $\sqrt{s}$  the smearing effect is somewhat enhanced over that shown in Fig. 1. The theoretical predictions are in qualitative agreement with the data

which can be seen to span the area between the solid and dashed curves at both values of  $\sqrt{s}$ . This agreement provides yet another consistency check on the theory.

The results shown in Figs. 1 and 2 indicate that high- $p_T$  direct photons are being observed in  $pp$  reactions at the level predicted by QCD. It should be noted that this conclusion does not depend sensitively on the assumptions used in the  $k_T$  smearing calculation since the  $k_T$  effects are less important here than in high- $p_T$  hadron production. In particular, the results of a calculation using off-shell kinematics<sup>17</sup> would lie between the solid and dashed curves and would also be in good agreement with the data.

Having demonstrated the agreement between the theoretical predictions and the available experimental data, we shall in the next section consider the predictions for  $\gamma$  + jet cross sections.

### III. $\gamma$ + JET CROSS SECTIONS

In the approximation that parton  $k_T$  effects can be neglected, the cross section for producing a jet opposite a direct photon is simply given by

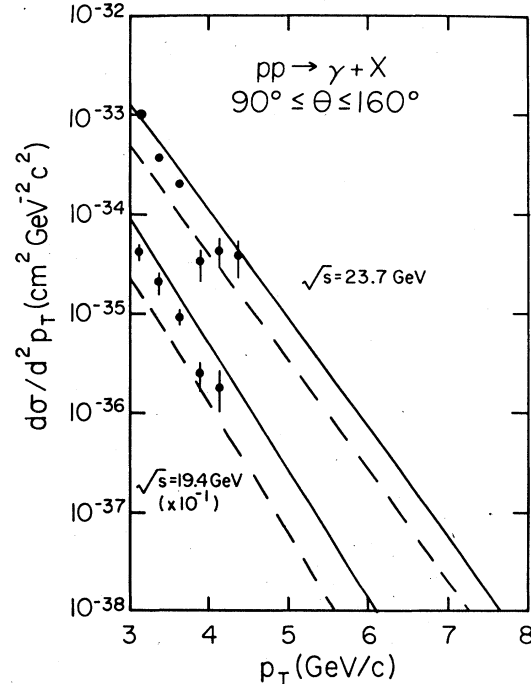


FIG. 2. A comparison between the theoretical predictions and the data for direct- $\gamma$  production integrated over the interval  $90^\circ < \theta < 160^\circ$ . The data are from Ref. 23. For clarity the curves and data at  $\sqrt{s}=19.4$  GeV have been suppressed by a factor of 10.

$$\frac{d\sigma(AB \rightarrow \gamma + \text{jet} + X)}{dy_1 dy_2 dp_T^2} = \sum_{ab} x_a x_b G_{a/A}(x_a, Q^2) G_{b/B}(x_b, Q^2) \frac{d\sigma}{dt}(ab \rightarrow \gamma + \text{jet}), \quad (4)$$

where  $x_{a,b} = \frac{1}{2}x_T(\cosh y_1 + \cosh y_2 \pm \sinh y_1 + \sinh y_2)$ ,  $y_1$  and  $y_2$  are the photon and jet rapidities, respectively, and  $x_T = 2p_T/\sqrt{s}$ . The parton-parton cross sections  $d\sigma/dt$  are given in Eq. (2).

As was shown in the previous section, parton  $k_T$  smearing can affect the single photon cross section, especially at moderate  $p_T$  values. However, with a trigger which depends on the sum of the magnitudes of the photon and jet momenta this dependency is greatly reduced. Such a trigger has been used in a previous jet experiment<sup>25</sup> and the decreased sensitivity of the theoretical cross section to parton  $k_T$  effects has been demonstrated in Ref. 26. The simplicity of Eq. (4) together with the fact that there are only two subprocesses to be considered here makes the  $\gamma$ +jet cross section a very attractive quantity to measure. The usefulness of the measurements outweighs, at least in part, the increased experimental problems associated with using a photon trigger.

In order to gain some insight into the structure of the  $\gamma$ +jet cross section the predictions for  $A p \rightarrow \gamma + \text{jet} + X$  are shown in Fig. 3 for  $A = \pi^+$ ,  $p$ , and  $\bar{p}$  with  $y_1 = y_2 = 0$  which corresponds to  $x_a = x_b = x_T$ . The  $pp$  reaction is almost totally dominated by the  $gq$  subprocess due to the smallness of the antiquark distribution in a proton. The  $gq$  subprocess in the  $\bar{p}p$  case is the same for the  $pp$  reaction so that the additional contribution to the cross section for the  $\bar{p}p$  reaction is coming from the  $q\bar{q}$  subprocess. This is reasonable since the  $\bar{p}$  has valence antiquarks. Now, pions also have valence antiquarks, but as is shown by the dashed and dash-dot lines, the  $gq$  subprocess dominates in the moderate- $p_T$  region for the  $\pi^-$  case and for all  $p_T$  values shown for the  $\pi^+$  case. The  $q\bar{q}$  subprocess is reduced by a factor of 4 in the  $\pi^+$  case compared to the  $\pi^-$  reaction because the valence antiquark is a  $\bar{d}$  as opposed to a  $\bar{u}$ . Of course, the  $gq$  contribution is the same for both the  $\pi^+$  and  $\pi^-$  cases. The dominance of the  $gq$  subprocess stems from the fact that for both pions and protons the gluon distribution is larger than the  $u$ -quark distribution in the region  $x \lesssim 0.5$ . Notice that for both the  $\pi^-$  and the  $\bar{p}$  reactions the  $q\bar{q}$  subprocess dominates for  $p_T \gtrsim 6$  in Fig. 3 which corresponds to  $x_T \gtrsim 0.4$ . This situation may be altered somewhat if a smaller gluon distribution in the proton or pion is used, but the situation is qualitatively unchanged.

The effects of the large gluon distributions in

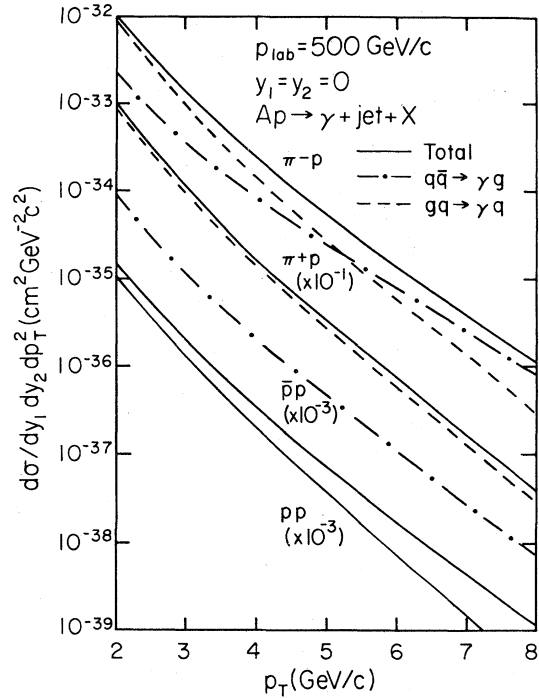


FIG. 3. Predictions for the  $\gamma$ +jet cross sections at  $p_{\text{lab}} = 500 \text{ GeV}/c$ . For clarity, the  $\pi^+p$  predictions have been suppressed by a factor of 10, and the  $pp$  and  $\bar{p}p$  predictions have been suppressed by a factor of 1000.

the pion and proton are further illustrated in Fig. 4 where away-side rapidity distributions are shown for the  $\pi^-$  reaction at two values of the photon rapidity. From these curves it is clear that at  $p_T = 3 \text{ GeV}/c$  the  $gq$  reaction is dominant over most of the available rapidity range. At high  $p_T$  values the  $q\bar{q}$  contribution grows relative to the  $gq$  term and begins to dominate over a larger region in  $y_2$ . This is illustrated in detail in Fig. 5 where the away-side rapidity distribution is shown for the  $\pi^-$  reaction at  $500 \text{ GeV}/c$  with  $y_1 = 0$  and  $p_T = 5 \text{ GeV}/c$ . Now a larger role is played by the  $q\bar{q}$  subprocess and, in fact, it is the dominant term for  $y_2 > 0.5$ . Comparison of Figs. 4 and 5 illustrates the point that the ratio of the  $q\bar{q}$  to  $gq$  contributions is largest in the region  $y_2 > 0$  for a given value of  $y_1$ . With  $y_1$  fixed,  $y_2 > 0$  corresponds to large  $x$  for the pion and small  $x$  for the target proton and vice versa for  $y_2 < 0$ . The slower falloff of  $G_{\bar{u}/\pi^-}$  at large  $x$  compared to  $G_{u/p}$  is the cause for the asymmetric shape of the  $q\bar{q}$  contribution about  $y = 0$ . This result means that the percentage of away-side gluon jets relative to the total number of events varies as a function of  $y_2$ . Let  $n_q$  and  $n_g$  denote the relative event rates corresponding to the  $gq$  and  $q\bar{q}$  subprocesses, respectively. Then the fraction of the total number of events which

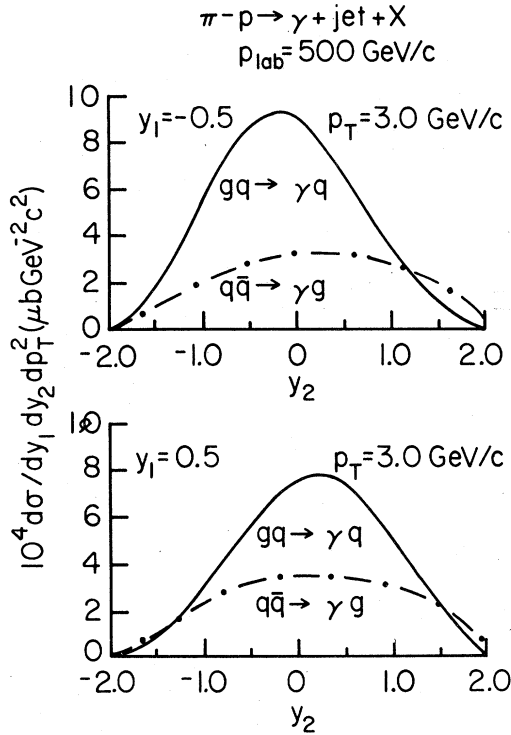


FIG. 4. Predictions for the away-side rapidity distributions in  $\pi^- p \rightarrow \gamma + \text{jet} + X$  at  $p_{\text{lab}} = 500 \text{ GeV}/c$  with  $p_T = 3 \text{ GeV}/c$  and  $y_1 = -0.5$  and  $0.5$ .

corresponds to a  $\gamma g$  final state is  $R_g = n_g / (n_q + n_g)$ .  $R_g$  is shown in Fig. 5 versus  $y_2$  at  $y_1 = 0$  and  $p_T = 5 \text{ GeV}/c$  and also versus  $p_T$  at  $y_1 = 0$  and  $y_2 = 1.0$ . The behavior discussed above is clear.  $R_g$  is largest at the extreme values of  $y_2$ , with  $y_2 > 0$  corresponding to a larger ratio than  $y_2 < 0$ , and  $R_g$  is the smallest near  $y = 0$ . In addition,  $R_g$  increases at fixed  $y_1$  and  $y_2$  as  $p_T$  is increased. Therefore, by varying  $p_T$ ,  $y_1$ , and  $y_2$  one can vary the percentage of gluon jets and then look for differences in the jet properties observed in regions where either quark or gluon jets are dominant. This may provide a means of discriminating between quark and gluon jets.

#### IV. PARTON-MODEL PHENOMENOLOGY

In this section a variety of results will be presented concerning the possible measurement of various distribution and fragmentation functions obtained by comparing the  $\gamma + \text{jet}$  cross sections for various beam particles, specifically  $\pi^+$ ,  $p$ , and  $\bar{p}$ . Also, a method of extracting the  $Q^2$  dependences of these functions will be presented. In the following it will be assumed that a double-arm trigger such as that discussed in the preceding section will be used. Therefore, possible parton

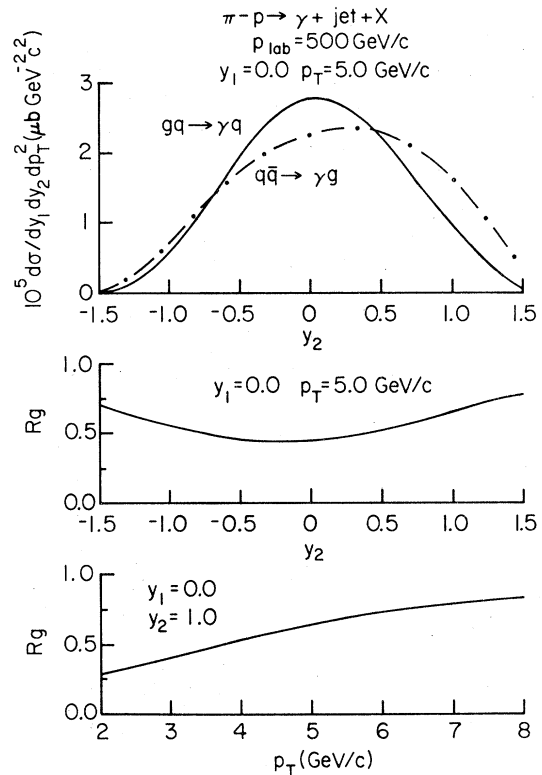


FIG. 5. Prediction for the away-side rapidity distribution for  $\pi^- p \rightarrow \gamma + \text{jet} + X$  at  $p_{\text{lab}} = 500 \text{ GeV}/c$  with  $p_T = 5 \text{ GeV}/c$  and  $y_1 = 0.0$ . Also shown are the predictions for the gluon-jet ratio  $R_g$  at  $y_1 = 0$ ,  $p_T = 5 \text{ GeV}/c$  and  $y_1 = 0$ ,  $y_2 = 1.0$ .

$k_T$  smearing effects will be minimized and, accordingly, such effects will be neglected hereafter.

#### A. Distribution functions

There are many advantages to be gained experimentally if one considers ratios of cross sections since, then, many systematic errors cancel out.<sup>25</sup> Therefore, define the ratio  $R_{ab}(x_a, x_b)$  by

$$R_{ab}(x_a, x_b) = \frac{d\sigma(a p \rightarrow \gamma + \text{jet} + X)}{dy_1 dy_2 dp_T^2} \bigg/ \frac{d\sigma(b p \rightarrow \gamma + \text{jet} + X)}{dy_1 dy_2 dp_T^2}, \quad (5)$$

where  $x_a$  and  $x_b$  have the same meaning as in Sec. III.

Both the  $\pi^+$  and  $p$  initiated reactions are dominated by the  $gq$  subprocess. In general, there will be two terms in the summation appearing in Eq. (3): one in which the gluon is from the beam particle and the quark is from the target particle and a second one in which the gluon and quark are interchanged. At low values of  $x$  the gluon distribution exceeds those of the various quarks while

the opposite is true at large  $x$ . Therefore, in the region of large  $x_a$  and small  $x_b$ , the term with the quark coming from the beam and the gluon coming from the target will dominate. Consider, then, the ratio  $R_{\pi^+p}$  in this region. After canceling all common factors one obtains the simple result

$$R_{\pi^+p} \approx F_2^{\pi^+}(x_a)/F_2^p(x_a), \quad (6)$$

where the structure functions  $F_2^A(x_a)$  are defined by analogy with electroproduction:

$$F_2^A(x) = \sum_{i=1}^{2f} e_i^2 x G_{q_i/A}(x). \quad (7)$$

The proton structure function is known from deep-inelastic scattering measurements and, therefore, one can extract the pion structure function. The question of the relevant value of  $Q^2$  at which these structure functions are measured will be discussed below.

The pion structure function defined in Eq. (7) can be written as follows if the contribution of sea quarks is neglected:

$$F_2^{\pi^+}(x) \approx \frac{5}{9} x G_{u/\pi^+}(x).$$

Notice that this method of measuring  $F_2^{\pi^+}$  (and, hence,  $G_{u/\pi^+}$ ) is cleaner than one employing a two-jet cross section<sup>25</sup> since in the latter case both the numerator and denominator contain linear combinations of quark and gluon distribution functions.

The next step is to measure the ratio  $R_{\pi^+p}$  at the symmetric point  $y_1 = y_2 = 0$  for which one has  $x_a = x_b = x_T$ . Then the ratio contains two terms:

$$R_{\pi^+p}(x_T, x_T) = \frac{1}{2} \frac{G_{u/\pi^+}(x_T)}{G_{g/p}(x_T)} + \frac{1}{2} \frac{F_2^{\pi^+}(x_T)}{F_2^p(x_T)}. \quad (8)$$

If the  $x_T$  range is chosen so as to overlap with the  $x_a$  range measured previously, then the second term is known and the first term may be extracted from the data. The ratio of the gluon distributions is interesting by itself, but one can go somewhat further.

Consider the  $pp$  reaction for which the cross section at  $y_1 = y_2 = 0$  is proportional to the gluon distribution in the proton. Using this, the *shape* of the distribution should be relatively easy to measure, although the *normalization* will be affected by questions of jet detection efficiency, cross-section normalization uncertainties, etc. However, having determined the shape of the gluon distribution from the  $pp \rightarrow \gamma + \text{jet} + X$  data, one can normalize it by using the deep-inelastic scattering data for the second moment of the distribution, i. e., normalize the gluon distribution so that the gluons carry 50% of the proton's momentum. Finally, then, one can use the resulting value for  $G_{g/p}(x)$  together with Eqs. (6) and (8) to obtain a

measurement of the gluon distribution in the pion.

As a check on the above procedure the ratio  $R_{\pi^+p}$  in the region where  $x_b$  is large and  $x_a$  is small will be given by

$$R_{\pi^+p} \approx G_{g/\pi^+}(x_a)/G_{g/p}(x_a).$$

Thus, in this region the cross-section ratio can be checked against the gluon-distribution ratio obtained from Eq. (8) provided that an overlapping region of  $x_a$  and  $x_T$  can be found. In actual practice, this last measurement will be restricted to rather small values of  $x_a$  where the difference in the power-law behaviors of the two-gluon distributions will not be readily apparent. However, the ratio can be used to check the relative normalization of the two-gluon distributions.

Next, consider the  $\pi^-$  and  $\bar{p}$  initiated reactions. As discussed previously, these reactions have comparable contributions from both the  $gq$  and  $q\bar{q}$  subprocesses. Therefore, ratio measurements analogous to the previous ones do not isolate specific distribution functions as easily. Furthermore, if the jet detection efficiencies are different for quark and gluon jets, then the contributions from the two terms will be altered. However, in principle one can predict the cross sections for  $\pi^-$  and  $\bar{p}$  beams given the distribution functions measured previously. Thus, data on these reactions provide a consistency check on the whole analysis.

In summary, measurements of the two reactions  $(\pi^+, p)p \rightarrow \gamma + \text{jet} + X$  in two special kinematic regions can be used, together with structure function data from deep-inelastic scattering, to extract values for the pion quark distributions and the pion and proton gluon distributions. Data taken with  $\pi^-$  and  $\bar{p}$  beams provide additional constraints and consistency checks on these functions.

## B. Fragmentation functions

Suppose that the hadronic-jet detector also has the capability of hadron identification and momentum measurement. Then, one can measure combinations of fragmentation functions for the away-side jet. Specifically, one can measure

$$\begin{aligned} \frac{d\sigma(AB \rightarrow \gamma + h + x)}{dy_1 dy_2 d\bar{p}_T^2 dz} &= \sum_{ab} x_a x_b G_{a/A}(x_a, Q^2) G_{b/B}(x_b, Q^2) \\ &\times \sum_j \frac{d\sigma}{dt}(ab \rightarrow \gamma + j) D_{h/j}(z), \end{aligned} \quad (9)$$

where  $y_2$  is still the away-side-jet rapidity and  $z$  is the fraction of the jet momentum taken by the hadron. Dividing Eq. (9) by Eq. (4), the  $\gamma + \text{jet}$  cross section, yields the normalized  $z$  distribu-

tion  $dN(h, A)/dz$  for a hadron  $h$  on the away-side produced from a beam  $A$ .

The expressions for the  $z$  distributions obtained using either  $\pi^+$  or  $p$  beams are very simple as a result of the fact that they are both dominated by the  $gq$  subprocess. Since the  $u$  quark is favored by a factor of 4 over the  $d$  quark one gets approximately

$$dN(h, \pi^+)/dz \simeq dN(h, p)/dz \simeq D_{h/u}(z).$$

There are minor corrections coming from the neglected terms which are easily calculated. For example, with a proton beam and keeping both  $u$  and  $d$  quarks one has

$$dN(\pi^+, p)/dz \simeq D_{\pi^+/u}(z)(4R + r^{-1})/(4R + 1)$$

and

$$dN(\pi^-, p)/dz \simeq D_{\pi^-/u}(z)(4R + r)/(4R + 1),$$

where  $R = G_{u/p}(x)/G_{d/p}(x)$  and  $r = D_{\pi^+/u}(z)/D_{\pi^-/u}(z)$ . Similar expressions can be derived for other hadron/beam combinations.

For the case of  $\pi^-$  or  $\bar{p}$  beams the extraction of quark fragmentation functions is more difficult. However, the presence of the  $q\bar{q} \rightarrow \gamma g$  subprocess allows for the possibility of extracting the gluon fragmentation functions. In order to obtain a more compact notation, let  $\sigma(A)$  and  $\sigma(A, h)$  denote the cross sections given in Eqs. (4) and (9), respectively. Then, the gluon fragmentation function into a hadron  $h$  can be obtained in at least two ways:

$$D_{h/g}(z) = \frac{1}{2} \frac{\sigma(\bar{A}, h) + \sigma(\bar{A}, \bar{h}) - \sigma(A, h) - \sigma(A, \bar{h})}{\sigma(\bar{A}) - \sigma(A)}, \quad (10)$$

where  $A = \pi^+$  or  $p$ .

Therefore, by identifying the hadrons in the away-side jet and measuring their momenta in reactions initiated by  $\pi^+$ ,  $p$ , and  $\bar{p}$  beams one can measure both quark and gluon fragmentation functions. Indeed, Eq. (10) may well represent one of the cleanest methods of measuring gluon fragmentation functions.

It should be noted that the above fragmentation function measurements can still yield useful information in the case where the charge of the away-side hadrons is measured, but not the particle type. Then what one obtains are sets of fragmentation functions averaged over particle types, but in practice pions will dominate.

One test for the presence of gluon jets which is often mentioned is to look for flavor independence among the fragments of the jet. Thus, if the  $q\bar{q} \rightarrow \gamma g$  subprocess is dominant, one might expect the away-side  $z$  distributions for positive and negative

particles to be equal. However, this can be misleading, especially for the case of  $\bar{p}$  beams. Using the two relations  $G_{q/p}(x) = G_{\bar{q}/\bar{p}}(x)$  and  $D_{h/q}(z) = D_{\bar{h}/\bar{q}}(z)$  it is easy to show that for the special case of  $y_1 = y_2 = 0$ , where  $x_a = x_b = x_T$ , the ratio of  $z$  distributions for positive and negative particles is identically 1 for the  $\bar{p}$  reaction independent of the relative contributions of the  $gq$  and  $q\bar{q}$  subprocesses. This same result is approximately true for the  $\pi^-$  case. Therefore, some caution must be used when employing this test in a search for gluon jets.

### C. $Q^2$ dependence

In the preceding discussion of distribution and fragmentation functions possible dependences on  $Q^2$  have been ignored. However, it is well known that QCD predicts logarithmic scaling violations for these functions. The basic problem associated with measuring a possible  $Q^2$  dependence is that in the leading-logarithm approximation there is no unique definition of  $Q^2$  relevant for high- $p_T$  scattering. Consider, for example, a measurement of  $F_2^z$  using Eq. (6) at fixed  $s$ . Varying  $x_a$  amounts to varying  $p_T$ ,  $y_1$ , and/or  $y_2$ . Thus,  $\hat{s}$ ,  $\hat{t}$ , and  $\hat{u}$  are all subject to change and, therefore,  $Q^2$  is varying. There is, however, at least one instance where the situation is less complex. At the symmetric point  $y_1 = y_2 = 0$  where  $x_a = x_b = x_T$  the subprocess Mandelstam variables become

$$\hat{s} = x_T^2 s$$

and

$$\hat{t} = \hat{u} = -\hat{s}/2. \quad (11)$$

The various expressions for  $Q^2$  which are often encountered in the literature then reduce to  $p_T^2$  with a coefficient of order one. Some examples are

$$Q^2 = \hat{s} \rightarrow 4p_T^2,$$

$$Q^2 = (\hat{s}\hat{t}\hat{u})^{1/3} \rightarrow 2.52p_T^2,$$

$$Q^2 = -\hat{t} \text{ or } -\hat{u} \rightarrow 2p_T^2,$$

$$Q^2 = 2\hat{s}\hat{t}\hat{u}/(\hat{s}^2 + \hat{t}^2 + \hat{u}^2) \rightarrow 4/3p_T^2.$$

On this basis it has been argued<sup>10</sup> that in this kinematic region a reasonable estimate of  $Q^2$  would be  $Q^2 \simeq 2p_T^2$ . Now, if one can obtain measurements at fixed  $p_T$  but different values of  $x_T$ , then  $x_a = x_b = x_T$  can be varied while  $Q^2$  is fixed. Note that  $Q^2$  will be fixed under these circumstances regardless of the coefficient of  $p_T^2$  used in its definition. The only ambiguity is in inferring the magnitude of the  $Q^2$  at which the measurement was performed.

Measurements of this type are particularly well suited to the determination of the fragmentation

functions as discussed above since those functions can be completely determined using data obtained with  $y_1=y_2=0$ . The structure function measurements are different, however, in that data from different angular regions must be compared and there is no way at present of ensuring that  $Q^2$  is the same for both sets of measurements.

### V. CONCLUSIONS

In this analysis we have shown that the present data on high- $p_T$  direct photons are consistent with predictions based on lowest-order QCD subprocesses. Next, the theoretical simplicity of reactions of the form  $AB \rightarrow \gamma + \text{jet} + X$  was stressed, especially when a double-arm trigger is used as this

helps to eliminate effects of parton  $k_T$  smearing. Such measurements can be used to determine the  $\pi^+$  quark distributions as well as the  $\pi^+$  and  $p$  gluon distributions when supplemented by proton-structure-function data from deep-inelastic scattering. Furthermore, if particle-identification and momentum-measurement capability exists for the away-side jet, then both quark and gluon fragmentation functions can be measured separately. Finally, it is possible to measure the  $Q^2$  dependence of these functions if the measurements are made over a range of  $s$  values at  $y_1=y_2=0$  with  $p_T$  fixed.

### ACKNOWLEDGMENT

This work was supported in part by the U. S. Department of Energy.

- 
- <sup>1</sup>For a recent review of the status of this field see *Proceedings of the 1979 International Symposium on Lepton and Photon Interactions at High Energies, Fermilab*, edited by T. B. W. Kirk and H. D. I. Abarbanel (Fermilab, Batavia, Illinois, 1980).
- <sup>2</sup>E. Witten, Nucl. Phys. **B120**, 189 (1977).
- <sup>3</sup>M. Fontannaz *et al.*, Phys. Lett. **89B**, 263 (1980).
- <sup>4</sup>J. F. Owens, Phys. Rev. D **21**, 54 (1980).
- <sup>5</sup>G. R. Farrar, Phys. Lett. **67B**, 337 (1977).
- <sup>6</sup>H. Fritsch and P. Minkowski, Phys. Lett. **69B**, 316 (1977).
- <sup>7</sup>F. Halzen and D. M. Scott, Phys. Rev. Lett. **40**, 1117 (1978); Phys. Rev. D **18**, 3378 (1978); **21**, 1320 (1980).
- <sup>8</sup>R. Rückl, S. J. Brodsky, and J. F. Gunion, Phys. Rev. D **18**, 2469 (1978).
- <sup>9</sup>R. Field, in *Quantum Chromodynamics*, proceedings of the La Jolla Institute, 1978, edited by W. Frazer and F. Henyey (AIP, New York, 1979), p. 97.
- <sup>10</sup>A. P. Contogouris, S. Papadopoulos, and M. Hongoh, Phys. Rev. D **19**, 2607 (1979).
- <sup>11</sup>P. Aurenche and J. Lindfors, Nucl. Phys. **B168**, 296 (1980).
- <sup>12</sup>G. R. Farrar and G. C. Fox, Nucl. Phys. **B167**, 205 (1980).
- <sup>13</sup>J. F. Owens and J. D. Kimel, Phys. Rev. D **18**, 3313 (1978).
- <sup>14</sup>R. D. Field, Phys. Rev. Lett. **40**, 991 (1978); R. P. Feynman, R. D. Field, and G. C. Fox, Phys. Rev. D **18**, 3320 (1978).
- <sup>15</sup>J. F. Owens and E. Reya, Phys. Rev. D **17**, 3003 (1978).
- <sup>16</sup>A. P. Contogouris, R. Gaskill, and S. Papadopoulos, Phys. Rev. D **17**, 2314 (1978).
- <sup>17</sup>W. E. Caswell, R. R. Horgan, and S. J. Brodsky, Phys. Rev. D **18**, 2415 (1978); R. Horgan and P. N. Scharbach, Phys. Lett. **81B**, 215 (1979).
- <sup>18</sup>J. F. Owens, in *Quarks, Gluons, and Jets*, proceedings of the XIV Rencontre de Moriond, edited by J. Tran Thanh Vân (Editions Frontières, Dreux, France, 1979), p. 229.
- <sup>19</sup>M. Diakonou *et al.*, Phys. Lett. **91B**, 296 (1980).
- <sup>20</sup>The preliminary data from the  $\overline{CCOR}$  collaboration are contained in Refs. 1 and 21.
- <sup>21</sup>M. J. Tannenbaum, review talk presented at the Annual Meeting of the Division of Particles and Fields, Montreal, 1979 (unpublished).
- <sup>22</sup>E. Amaldi *et al.*, Nucl. Phys. **B150**, 326 (1979).
- <sup>23</sup>R. M. Baltrusaitis *et al.*, Phys. Lett. **88B**, 372 (1979).
- <sup>24</sup>R. M. Baltrusaitis *et al.*, Phys. Rev. Lett. **44**, 122 (1980).
- <sup>25</sup>M. D. Corcoran *et al.*, Phys. Rev. Lett. **41**, 9 (1978); M. Dris *et al.*, Phys. Rev. D **19**, 1361 (1979).
- <sup>26</sup>J. F. Owens, Phys. Rev. D **20**, 221 (1979).